Dopant binding energies in P-doped Ge[110] nanowires using real-space pseudopotentials

Alex J. Lee

Department of Chemical Engineering, University of Texas at Austin, Austin, Texas 78712, USA

Tzu-Liang Chan

Department of Physics, Hong Kong Baptist University, Kowloon Tong, Kowloon, Hong Kong

James R. Chelikowsky

Center for Computational Materials, Institute for Computational Engineering and Sciences,
and Departments of Physics and Chemical Engineering, University of Texas at Austin, Austin, Texas 78712, USA

We apply a real-space pseudopotential formalism for charged one-dimensional periodic systems to examine the binding energies of P dopants in Ge[110] nanowires with varying periodicities and diameters. Binding energies calculated by density functional quasiparticle energies of the neutral dopant are severely underestimated whereas those calculated by quasiparticle energies of the ionized defect are overestimated. We find the best method for determining binding energies is to adopt a composite approach that evaluates the total energy difference between charged and neutral systems for the ionization energy of the P dopant, but uses the quasiparticle energy for the electron affinity of the pure Ge nanowire. Our formalism offers a simple density functional method for calculating dopant binding energies of small nanowire systems without the use of computationally intensive many-body perturbation theory calculations.

I. INTRODUCTION

The dopant binding energy (alternatively referred to in the literature as the dopant ionization or activation energy) is an important property for understanding and evaluating semiconductor performance as it relates to the doping efficiency. For nanostructures, experimental and theoretical studies have shown that the binding energy increases with decreasing size owing to dielectric mismatch and quantum confinement, potentially moving a shallow defect into a deeper state, which can have drastic effects on device functionality [1–5]. However, significant discrepancies between theoretical models exist, particularly in the magnitude of the binding energy [5,6], and a more accurate modeling of the defect states will lead to a better understanding of the properties that drives novel technological devices such as functionally doped semiconductor nanowires. Some applications for doped nanowires include biological and chemical sensors, thermoelectrics, and photovoltaics [7–9].

For a donor in a nanowire, the binding energy E_b is defined as the energy needed to ionize a neutral dopant and move its electron to the conduction band edge far away, evaluated by $E_b = I_d - A_p$, where I_d and A_p refer to the ionization energy and electron affinity of the doped and pure (or intrinsic) system respectively. These two quantities can be calculated from total energy differences between the appropriate charged and neutral systems (ΔSCF). For periodic systems such as nanowires, the energy calculation of a charged system is problematic owing to the long-range Coulomb force, which adds an artificial interaction via its repeated image and causes its total energy to diverge. Typical supercell calculations of charged systems introduce a compensating charge background (or jellium) to screen this long-range interaction. However, the charge background itself interacts with the system and introduces its own artificialities. Numerous schemes have been devised to correct for this interaction to model accurately the energy and potential of a charged material, including the well-known Makov-Payne scheme [10–13]. These schemes may require very large supercells to obtain converged results, which can be computationally intensive [14].

We will apply an alternative, computationally competitive approach to calculate dopant binding energies in P-doped Ge[110] nanowires. Compared to Si, Ge features a lower band gap and a shallower defect state for P in the bulk [15]. Quantum confinement effects are expected to differ in Ge compared to Si owing to the larger Bohr exciton radius of 24.3 nm in Ge compared to 4.9 nm in Si [16,17]. Thus, the properties of doped Ge may be more flexible and easily tuned for various electronic applications. Our theoretical approach is based on real-space pseudopotentials constructed within density functional theory (DFT). The charged nanowire is confined within a one-dimensional periodic supercell along the wire axis. Unlike a three-dimensional periodic supercell interwire interactions are eliminated, and total energy corrections related to such interactions can be avoided. In addition it is no longer necessary to include a large amount of vacuum space to converge the total energy of a charged nanowire (~5 Å is needed), which alleviates the computational demand. The interaction between image cells along the wire axis can be addressed without introducing a compensating charge background that interacts with the system itself by defining an appropriate electrostatic boundary condition for the Kohn-Sham equation. This approach has been used to examine the capacitance of metallic and semiconductor nanowires [18]. Details of the formalism are outlined in a previous paper [19].

The dopant binding energy (E_b) can also be obtained by calculating ionization energies (I_d) and electron affinities (A_p) as quasiparticle energies based on the highest occupied (HOMO) and lowest unoccupied (LUMO) Kohn-Sham eigenvalues. This "quasiparticle approximation" is known to have

issues within DFT, in part because Kohn-Sham eigenvalues have an ambiguous physical interpretation owing to the delocalization of electrons, and also because DFT underestimates the HOMO-LUMO band gap. Screening charges around the ionized dopant are not accounted for by the HOMO eigenvalue. Considering this shortcoming, Niquet *et al.* [6] proposed that E_b with DFT using the quasiparticle approach can be better approximated by $E_b = A_d(+) - A_p(0)$. Here, $A_d(+)$ is the electron affinity of the ionized doped system obtained from the LUMO eigenvalue after the doped system is ionized, while $A_p(0)$ is still obtained from the LUMO eigenvalue of the corresponding neutral system of pure Ge. That is, I_d is approximated by $A_d(+)$ such that the interaction effects following ionization can be included. In this paper, both the original quasiparticle and Niquet's approach will be evaluated and compared with the ΔSCF approach. For nanowires, while the original quasiparticle approach does not take into account the interaction between the screening charges and the wire surface, we found that Niquet's approach double-counts it. It is best to adopt a composite approach to determine E_b using the total energy difference to calculate I_d but the quasiparticle approach to calculate A_p.

II. COMPUTATIONAL METHODS

Electronic structure calculations were carried out using PARSEC, a pseudopotential code for DFT calculations in real-space without the use of an explicit basis set [20–23]. The pseudopotential used for Ge is based on the Troullier-Martins [24] construction with valence configuration $4s^2 4p^2 4d^0$. Partial core corrections are included and p is adopted as the local component [25]. This pseudopotential has been used in previous studies on Ge nanowires and provides accurate results for the wire's mechanical and electronic properties [26,27]. Exchange correlation was handled using Ceperley-Alder, a functional based on the local density approximation (LDA) [28]. Structural relaxations were performed using the BFGS method [29–32] with a force tolerance of ∼0.01 Ry/bohr. Only the Γ point was used for k-point sampling as the nanowires examined in the study had relatively large periodicities. Spin polarization was included for systems with unpaired electrons.

Figure 1 illustrates one of the Ge nanowires examined in the study. Wires were constructed along the [110] growth direction, as that orientation was shown to be the most energetically stable for small wires [33] and features some of the more interesting and well-researched electronic properties. Surface atoms were passivated with hydrogen capping atoms [34]. Nanowires were doped by substituting one of the innermost Ge atoms with a phosphorus atom, creating an n-type donor. We constructed and performed calculations on wires of diameter 1.16, 2.28, and 3.42 nm, where the diameter was defined as the smallest cylinder that can enclose the wire.

III. INTERACTION AMONG P DOPANTS

Since our goal is to study the isolated P dopant, we first examined the dependence of the formation energy E_{form}, ionization energy I_d, and electron affinity A_p on the periodicity of the Ge nanowire. This allows us to assess the interaction between P dopants from the periodic images along the wire
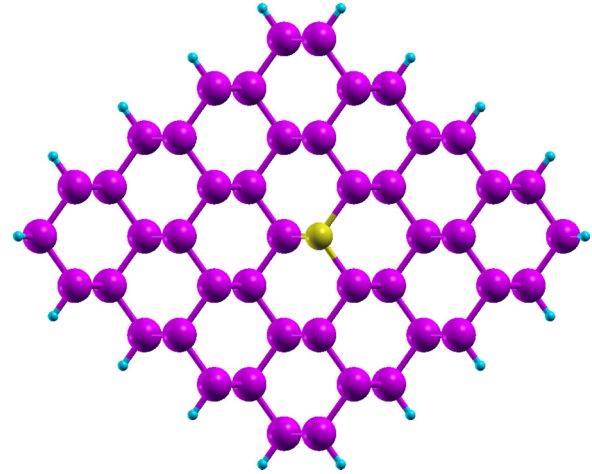
FIG. 1. (Color online) Axial view of a H-passivated P-doped Ge[110] nanowire with $D = 2.28$ nm. The smaller, lighter colored atom near the center is the P dopant. The small atoms at the surface of the wire are hydrogen capping atoms.

axis. Understanding the behavior of I_d and A_p is particularly important since they determine the binding energy E_b. The nanowire with a diameter $D = 1.16$ nm was chosen for this study. Structural relaxation was not used to ensure trends resulted from changes in periodicity only.

Formation energies were calculated by

$$E_{\text{form}}(P) = E(P - Ge) - E(Ge) + \mu(Ge) - \mu(P), \quad (1)$$

where $E(P - Ge)$ and $E(Ge)$ refer to the total energies of the P-doped and pure Ge wire, and $\mu(Ge)$ and $\mu(P)$ refer to the respective atom's chemical potential. The value for $\mu(Ge)$ was taken to be the energy per atom of bulk Ge, and $\mu(P)$ corresponded to the total energy of an isolated P atom. Similar choices for the chemical potentials were used in previous works on doped nanostructures [35,36].

In practice the chemical potentials depend on experimental conditions, which may not correspond to the theoretical values adopted here. However, we are only interested in the trend of E_{form}, not in their absolute values. We used a grid spacing of 0.47 a.u., which converges formation energies to within 0.05 eV. The results in Fig. 2(a) show that E_{form} increases with periodicity and quickly converges at a periodicity of 23.9 Å. The attractive interaction (∼1.3 eV) between P dopants from adjacent image cells quickly diminishes beyond a few Ge bond lengths. Beyond six times the length of the primitive cell, P dopants between image cells are essentially noninteracting, which is comparable to that in P-doped Si nanowires [36].

Figure 2(b) plots the behavior with periodicity for both $I_d(\Delta)$ and $A_p(\Delta)$, with Δ indicating that values were calculated as total energy differences between the appropriate charged and neutral systems. A grid spacing of 0.6 a.u. was used, which converges both quantities to within 0.01 eV. The $I_d(\Delta)$ curve looks similar to that of P-doped Si nanowires [19], which is expected since the ionization energies for Si and Ge nanocrystals were found to be similar [37]. The main characteristic is that $I_d(\Delta)$ increases with decreasing periodicity. Note that since the charged nanowire is enclosed within a cylindrical domain, interwire interactions are
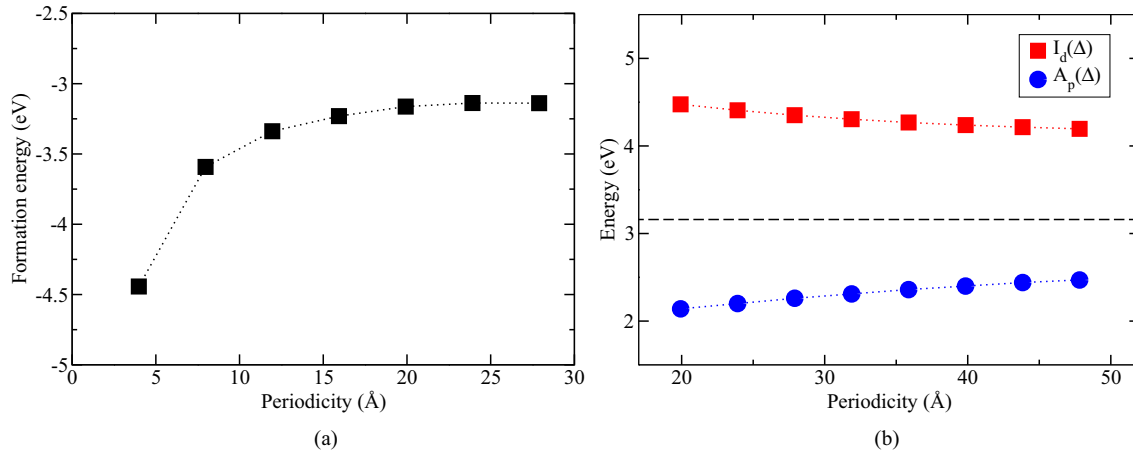
FIG. 2. (Color online) (a) The trend of E_{form} of a P dopant in a Ge[110] nanowire ($D = 1.16$ nm) with periodicity. (b) $I_d(\Delta)$ of the same P-doped Ge nanowire in (a) and $A_p(\Delta)$ of the corresponding pure Ge nanowire calculated by total energy differences (ΔSCF). The dashed line corresponds to $|\epsilon_{\text{CBM}}|$, which is the magnitude of the eigenvalue of the CBM of the pure Ge nanowire. $A_p(\Delta)$ should converge to $|\epsilon_{\text{CBM}}|$ for large periodicities.

eliminated. Furthermore, although the nanowire repeats periodically along its axis, electrostatic intrawire interactions between image cells are also removed by selecting an appropriate reference vacuum level [19]. Therefore, the observed trend in Fig. 2(b) corresponds to interactions between unit cells that are nonelectrostatic in nature. According to a previous study on P-doped Si[110] nanowires, an induced surface charge forms when the P dopant is ionized. The repulsive interaction between the induced charges in adjacent image cells increases with smaller periodicity leading to a higher $I_d(\Delta)$ [19].

Compared to $I_d(\Delta)$, the $A_p(\Delta)$ decreases concurrently with periodicity. The electron affinity corresponds to the energy gain of a free electron placed in the conduction band minimum (CBM) of a pure Ge nanowire. In contrast to the localized P defect state, the CBM of the pure Ge wire is an extended state. The calculation of $A_p(\Delta)$ should correspond to putting an electron into a supercell of infinitely large periodicity. Using a smaller periodicity for the calculation thus confines the added electron to a finite region and consequently reduces $A_p(\Delta)$. It is expected that $A_p(\Delta)$ trends to $|\epsilon_{\text{CBM}}|$, where ϵ_{CBM} is the eigenvalue of the CBM for the pure Ge nanowire. A DFT study on a large Si nanocrystal suggests that $A_p(\Delta)$ converges to the CBM of bulk Si [38].

IV. QUANTUM CONFINEMENT EFFECTS

The effect of quantum confinement on the binding energy E_b of an isolated P dopant in a Ge[110] nanowire was examined by studying E_b versus wire diameter D. While the interaction between neutral P dopants diminishes beyond $\sim$24 Å, the interaction between ionized dopants is long ranged. In order to minimize the effect of having a finite periodicity, the wire periodicity is set to be 47.82 Å. At this length, the dispersion of the dopant band is less than 15 meV. Relaxed structures were obtained using a force tolerance of $\sim$0.01 Ry/bohr.

The binding energy $E_b(\Delta) = I_d(\Delta) - A_p(\Delta)$ can be calculated solely through total energy differences, where both $I_d(\Delta)$ and $A_p(\Delta)$ are calculated from the total energies of the

appropriate charged and neutral systems. This approach to calculate binding energies is known as ΔSCF. As discussed in the previous section, $I_d(\Delta)$ includes the quantum mechanical effects following the ionization of P, but these effects are expected to be slightly overestimated due to the finite periodicity of the wire. Figure 3(b) shows that $I_d(\Delta)$ is insensitive to D as the curve is quite flat. A similar trend was observed in P-doped Si nanocrystals [39,40] and nanowires [18]. The value for $I_d(\Delta)$ ($\sim$4.15 eV) is similar to that of a P-doped Si nanowire ($\sim$4 eV) [19]. This is to be expected since the ionization energies of Si and Ge nanocrystals are nearly identical [37]. The trend of $A_p(\Delta)$ decreases concurrently with D owing to quantum confinement on the CBM of the pure Ge nanowire. The resultant $E_b(\Delta)$ is plotted in Fig. 3(a), which shows an increasing trend with smaller D. The bulk value of E_b for P in Ge is $\sim$13 meV, indicating a a shallow dopant state [41]. For the nanowires examined in the study, the dopants are no longer shallow owing to the effects of dielectric mismatch and quantum confinement as observed in various experimental and theoretical studies on doped semiconductor nanostructures [1–5].

Since $I_d(\Delta)$ does not vary much with size, the variation of $E_b(\Delta)$ is mainly contributed by $A_p(\Delta)$. Therefore, the accuracy of $A_p(\Delta)$ is crucial as far as the trend of $E_b(\Delta)$ is concerned. Due to the imposed periodicity, $A_p(\Delta)$ was found to be underestimated in the pure Ge nanowire (see Fig. 2). As a result, determined values for $E_b(\Delta)$ are too high. It is essential to calculate the ionization energy based on ΔSCF in order to capture the polarization energy following dopant ionization. However, it is more accurate to calculate the electron affinity using a quasiparticle approach such that the effect of imposed periodicity is minimized. The quasiparticle approach calculates A_p using $|\epsilon_{\text{CBM}}|$. We denote the resultant electron affinity as $A_p(0)$ to indicate that the eigenvalue was taken from the neutral system. For the range of D examined, $A_p(\Delta)$ and $A_p(0)$ differ by $\sim$0.6 eV, but Fig. 3(b) shows that the difference narrows with larger D. We suggest a composite approach to calculate the binding energy by $I_d(\Delta) - A_p(0)$. While the effect of quantum confinement is significant in Ge nanowires with small D, the enhancement in the binding
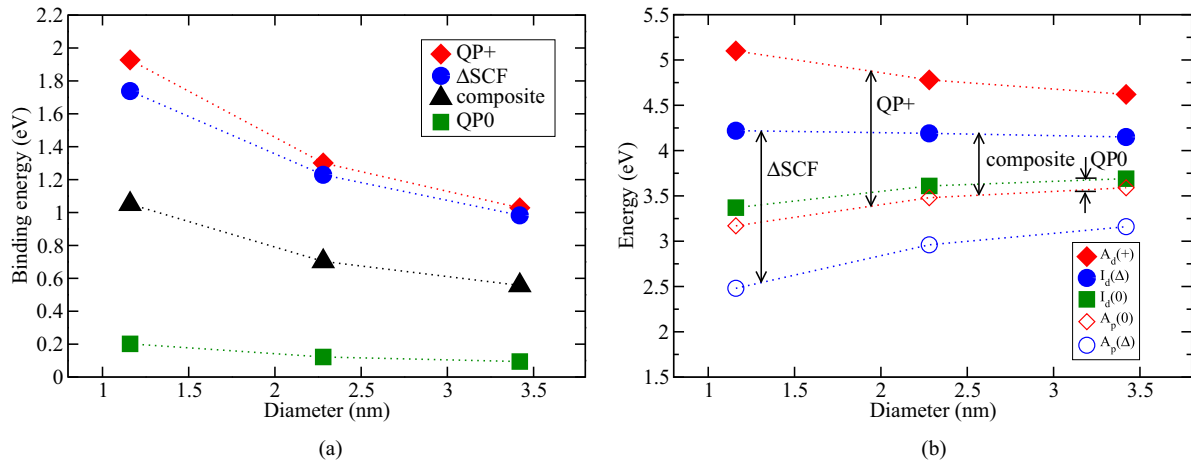
FIG. 3. (Color online) (a) The variation of E_b in a P-doped Ge[110] nanowire with respect to wire diameter D using various methods. (b) The corresponding variations of I_d and A_p with D. The different approaches to calculate E_b are shown in the legend. See the text for details on the methods.

energy should not be as large as predicted by $E_b(\Delta)$ but reduced by roughly half as in the composite method.

Both the ΔSCF and composite methods use total energies to compute the binding energy. It is also possible to evaluate E_b using solely a quasiparticle approach. In addition to $A_p(0)$, the ionization energy can be calculated using $|\epsilon_{\text{defect}}|$, where ϵ_{defect} is the eigenvalue of the P defect level within the gap of the Ge nanowire. We denote this ionization energy $I_d(0)$. In Fig. 3(b), $I_d(0)$ decreases with decreasing D as in $A_p(0)$. This behavior can be understood using the hydrogenic model of a shallow dopant in a semiconductor [15], which states that the trend of the defect level follows that of the semiconductor's CBM. The corresponding binding energy is $E_b(0) = I_d(0) - A_p(0)$ as illustrated in Fig. 3(a). We call this method QP0 to indicate that the ionization energy is calculated using the quasiparticle of the neutral doped system. $E_b(0)$ is severely underestimated compared to the ΔSCF methods owing to DFT's self-interaction error that results in an incorrect description of the energy levels in the conduction band. Similar issues were observed in P-doped Si nanowires using similar methods and functionals [5,6]. The DFT error is a relatively minor issue in the ΔSCF approach since the total energies of ground states are generally accurate when the system does not involve highly localized electronic states. The underestimate of $E_b(0)$ also originates from the lack of accounting by $I_d(0)$ for the energy associated with polarization after the dopant is ionized. This should not be a significant concern for $A_p(0)$ since the CBM is not a localized state, so the energy associated with polarization should be relatively small.

Noting the shortcomings of the QP0 approach, Niquet *et al.* suggested an alternative method that uses the ionized doped nanowire instead of the neutral system. They used the LUMO eigenvalue of the ionized system [denoted by $A_d(+)$] as the ionization energy of the neutral nanowire. This way the polarization energy associated with screening following dopant ionization is taken into account. The binding energy thus becomes $E_b(+) = A_d(+) - A_p(0)$. We call this approach QP+ to indicate that the ionization energy is calculated by a quasiparticle approach that uses an ionized dopant. The calculated $A_d(+)$ vs D in Fig. 3(b) shows that the effect of

screening is exaggerated by QP+ as $A_d(+)$ values are too high compared to $I_d(\Delta)$.

We found that the $I_d(\Delta)$ values are almost exactly the average of $I_d(0)$ and $A_d(+)$, or

$$A_d(+) \approx I_d(\Delta) + [I_d(\Delta) - I_d(0)] . \qquad (2)$$

If $I_d(\Delta)$ is taken to be accurate, then $I_d(\Delta) - I_d(0)$ corresponds to the error of $I_d(0)$; thus $A_d(+)$, which was supposed to account for this error, ends up double-counting it. Using the expression for $A_d(+)$ in Eq. (2), it can be shown that $E_b(+) \approx E_b(\Delta) + [E_b(\Delta) - E_b(0)]$. Therefore, Niquet's QP+ method, which was devised to correct for the underestimate of E_b by the QP0 method, turns out to overestimate the binding energies as illustrated in Fig. 3(a).

One of the key differences between the QP0, QP+, and ΔSCF methods comes from the treatment of the ionization energy I_d of the doped system. A similar comparison between the magnitudes of I_d using these methods can be found in a study on small Na clusters [42]. In this study, ionization energies were calculated with LDA as well as with many-body perturbation theory (MBPT), including self-consistent GW (scGW). In the LDA results, $I_d(0)$ calculated from the HOMO of the neutral species were underestimated, and $I_d(+)$ calculated from the LUMO of the ionized species were overestimated, but $I_d(\Delta)$ calculated as total energy differences gave results closest to experimental values, being slightly overestimated by a few tenths of an eV. The LDA results for $I_d(\Delta)$ are reasonably close to the scGW results, often within 0.1 eV. Another study on small Ge clusters that compares ionization energies calculated by LDA and GW reports similar findings, where the LDA results for $I_d(\Delta)$ are slightly overestimated and those for $I_d(0)$ are grossly underestimated [43]. The study also computes electron affinities and finds that those calculated by LDA with the ΔSCF method are overestimated by a similar amount compared to GW and experimental results.

The composite method $E_b(\text{composite}) = I_d(\Delta) - A_p(0)$ thus adopts $I_d(\Delta)$ but continues to treat $A_p(0)$ using the quasiparticle approach, which is appropriate for an extended state (the CBM of the pure Ge nanowire) in order to mitigate
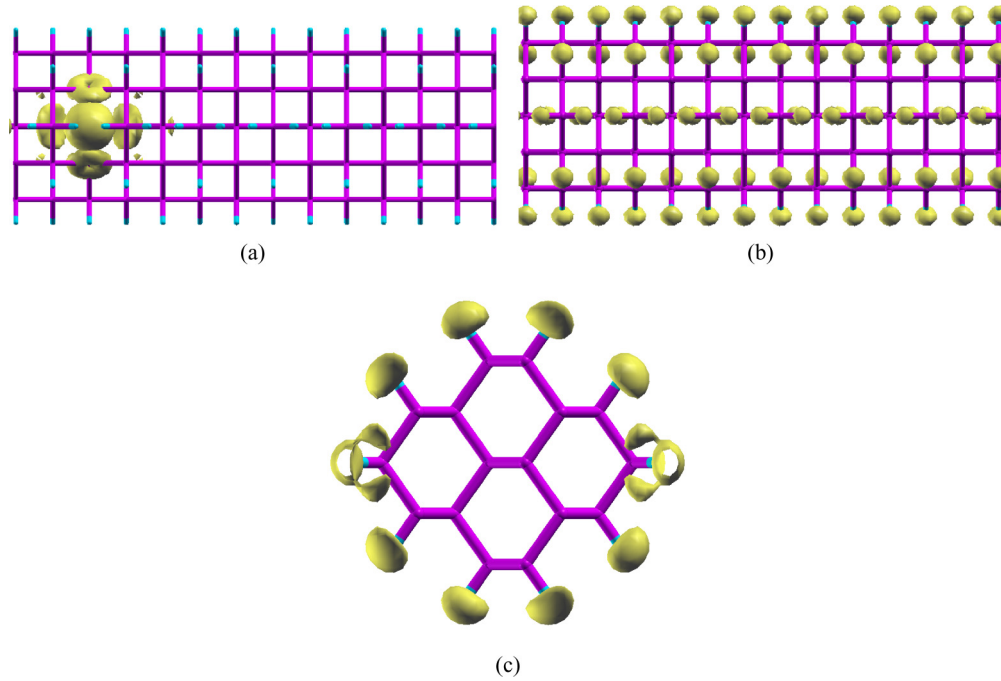
FIG. 4. (Color online) Surface contour plots for the induced charge density ρ_{ind} of various Ge nanowires ($D = 1.16$ nm). The contour surface corresponds to a chosen positive value of ρ_{ind}. Only the atomic bonds are drawn; individual atoms are not shown. (a) Side view of $\rho_{\mathrm{ind}}(\mathrm{P})$ for the ionized P-doped wire. The $\rho_{\mathrm{ind}}(\mathrm{P})$ is localized around the P atom. (b) Side view of $\rho_{\mathrm{ind}}(\mathrm{Ge})$ for the negatively charged pure Ge wire. In contrast to (a), $\rho_{\mathrm{ind}}(\mathrm{Ge})$ is spread evenly throughout the wire. (c) Axial view of (b). The $\rho_{\mathrm{ind}}(\mathrm{Ge})$ is spread around the surface of the wire at $r \approx 6$ Å.

the effects of imposing periodicity. The most accurate result for the binding energy should correspond to the composite method, where QP0 underestimates the binding energies while ΔSCF and QP+ overestimate them. The differences between the various methods become less significant for larger wires. Ideally, the various methods should be benchmarked against MBPT since the study of defects involves the energy band gap, which LDA has problems reproducing; however, we could not find a relevant MBPT study for our system.

To attain a deeper understanding of the charged nanowires, we examined the induced charge ρ_{ind} of the ionized P-doped and the negatively charged pure Ge nanowire ($D = 1.16$ nm). The induced charge density of the ionized P-doped nanowire [$\rho_{\mathrm{ind}}(\mathrm{P})$] was obtained by taking the difference between the charge density of the ionized (positively charged) P-doped nanowire and that of the neutral undoped wire. The induced charge density of the negatively charged pure Ge wire [$\rho_{\mathrm{ind}}(\mathrm{Ge})$] was obtained by taking the difference between the charge density that corresponds to the first N electrons of the charged pure wire (with $N + 1$ electrons) and that of the neutral pure wire (with N electrons). As spin polarization was included for systems with unpaired electrons, the relative contributions to the charge density of the up and down spin states were weighted by their occupancies. In each case the charged density has the same number of electrons (N) such that ρ_{ind} corresponds to zero net charge. A positive (negative) ρ_{ind} indicates an excess (deficiency) of electrons compared to the neutral system.

Surface contour plots of $\rho_{\mathrm{ind}}(\mathrm{P})$ and $\rho_{\mathrm{ind}}(\mathrm{Ge})$ are shown in Fig. 4. The contour surface corresponds to a chosen positive value of ρ_{ind}. The plots show that $\rho_{\mathrm{ind}}(\mathrm{P})$ is localized around

the P dopant [Fig. 4(a)] whereas $\rho_{\mathrm{ind}}(\mathrm{Ge})$ is evenly spread throughout the wire axis [Fig. 4(b)]. This originates from the fact that the P defect state is localized whereas the CBM of the pure Ge wire is an extended state.

The radial variation of $\rho_{\mathrm{ind}}(\mathrm{P})$ and $\rho_{\mathrm{ind}}(\mathrm{Ge})$ was calculated in ~10 Å segments along the wire axis. Figure 5(a) plots a segment that contains the P dopant (located at $x \approx 5$ Å) whereas Fig. 5(b) plots a segment of the wire far from the P dopant ($x \approx 19$–29 Å). In the ionized P-doped wire, the electrons that screen the positive P ion are mostly drawn from around the surface of the nanowire, reflected in the figure as a deficiency of electrons [negative $\rho_{\mathrm{ind}}(\mathrm{P})$] at $r \approx 6$ Å. Since the DFT eigenvalue of the defect level $\epsilon_{\mathrm{defect}}$ does not capture such polarization effects, it is vital to calculate I_d using the ΔSCF approach. The electron deficiency at the wire surface extends to the segment far from the P dopant although $\rho_{\mathrm{ind}}(\mathrm{P})$ decreases in magnitude. The $\rho_{\mathrm{ind}}(\mathrm{P})$ on the nanowire surface leads to a repulsive interaction between periodic cells that results in an enhanced I_d as described in Sec. III. For the charged pure Ge wire, since the electron is added to an extended state, the radial variation of $\rho_{\mathrm{ind}}(\mathrm{Ge})$ is independent of the chosen segment along the wire axis (the $x \approx 19$–29 Å segment is plotted). In this case Fig. 5(b) shows an excess of electrons around the surface of the nanowire at $r \approx 6$ Å. This is also depicted in the surface contour plot of $\rho_{\mathrm{ind}}(\mathrm{Ge})$ in Fig. 4(c). Note that the $\rho_{\mathrm{ind}}(\mathrm{Ge})$ plots correspond to a finite linear charge density along the pure Ge nanowire. In contrast to the ionized P-doped wire, a single electron deposited into the CBM of an infinitely long pure Ge nanowire should not lead to a considerable ρ_{ind} as indicated. Therefore, the electron affinity should be well approximated by ϵ_{CBM}.
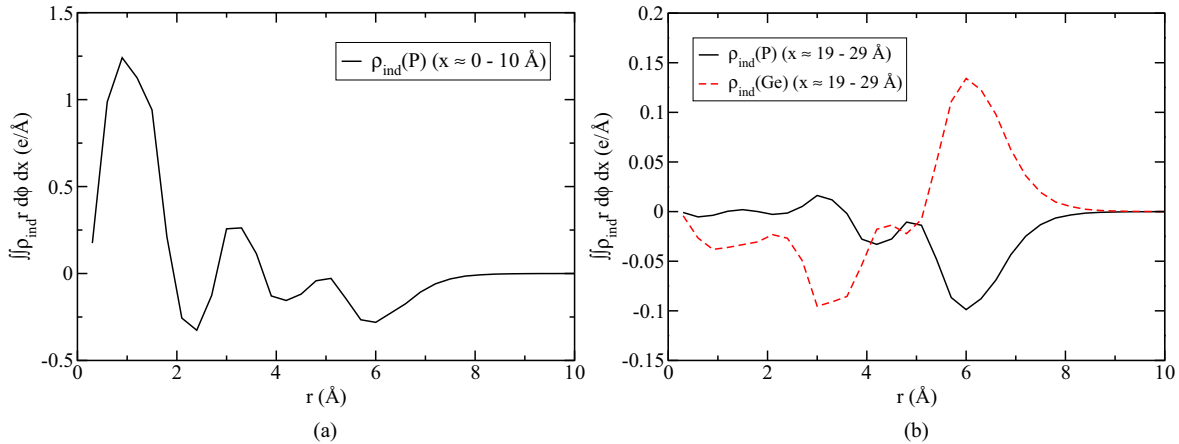
FIG. 5. (Color online) (a) The radial variation of $\rho_{\text{ind}}(\text{P})$ for the ionized P-doped Ge wire in a $\sim$10 Å segment along the x axis that contains the P dopant (located at $x \approx 5$ Å). (b) Same as in (a) but for a segment far from the P dopant ($x \approx 19$–29 Å). For the same segment, $\rho_{\text{ind}}(\text{Ge})$ for a charged pure Ge nanowire is also plotted for comparison.

While the effect of quantum confinement on E_b should involve $I_d(\Delta)$, the formation energy $E_{\text{form}}(\text{P})$ obtained from relaxed structures can be correlated to $I_d(0)$. Figure 6 plots $E_{\text{form}}(\text{P})$ as a function of D and shows that the magnitude of $E_{\text{form}}(\text{P})$ decreases concurrently with D. Since $|E_{\text{form}}(\text{P})|$ represents the energy of replacing a Ge atom with P, the trend implies that the nanowire becomes more difficult to dope as it becomes smaller. A similar "self-purification" effect has also been observed in doped Si nanostructures [35,44]. The eigenvalue of the defect level ϵ_{defect} [or $-I_d(0)$] is also plotted [it is by coincidence that the ϵ_{defect} are aligned with the $E_{\text{form}}(\text{P})$ without introducing a shift]. Its trend with D follows that of $E_{\text{form}}(\text{P})$ quite well, which provides evidence that the energetics of a shallow dopant in a nanostructure can be correlated with the Kohn-Sham eigenvalues of the dopant defect level [36].

V. CONCLUSIONS

We used our real-space DFT formalism for charged one-dimensional periodic systems to calculate and compare the
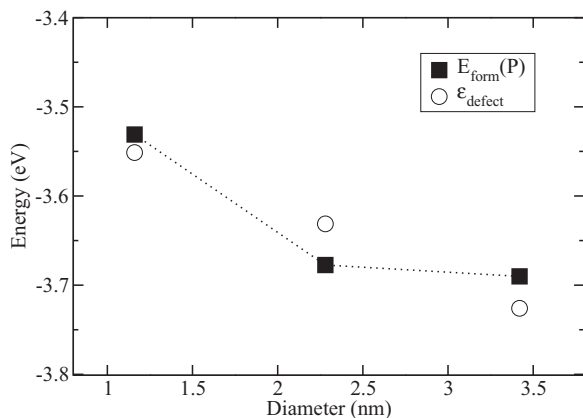
FIG. 6. The formation energy $E_{\text{form}}(\text{P})$ of doping P into a Ge[110] nanowire as a function of wire diameter D. Relaxed structures were used for the calculations. The eigenvalue of the dopant defect level $\epsilon_{\text{defect}} = -I_d(0)$ is also shown.

results of the dopant binding energy E_b with respect to wire diameter for a P dopant in a Ge[110] nanowire using various methods. For all sizes of nanowire examined, dopant levels are not shallow as in the bulk. Binding energies calculated using quasiparticle energies (QP0) of the neutral dopant are underestimated owing to the lack of accounting for the polarization energy associated with screening the ion, resulting in too shallow dopant levels. Conversely, the quasiparticle energies of the ionized defect (QP+) overestimate the binding energy because the polarization energy is double counted. Binding energies calculated by total energy differences (ΔSCF) between charged and neutral systems also overestimate the binding energy, and the error originates from the imposed periodicity of the wire. Our proposed composite method calculates the ionization energy $I_d(\Delta)$ of the P dopant by total energy differences, but calculates the electron affinity $A_p(0)$ of the pure Ge nanowire using a quasiparticle approach. Such a composite approach to calculate the binding energies likely gives the most accurate results. The study explores how our formalism for modeling charged 1-D periodic systems without a compensating charge background can be used to provide a computationally efficient DFT method for determining dopant binding energies in nanowires.

[1] M. T. Björk, H. Schmid, J. Knoch, H. Riel, and W. Riess, Nat. Nanotechnol. **4**, 103 (2009).

[2] J. Yoon, A. M. Girgis, I. Shalish, L. R. Ram-Mohan, and V. Narayanamurti, Appl. Phys. Lett. **94**, 142102 (2009).

[3] M. Diarra, Y. M. Niquet, C. Delerue, and G. Allan, Phys. Rev. B **75**, 045301 (2007).

[4] B. Li, A. F. Slachmuylders, B. Partoens, W. Magnus, and F. M. Peeters, Phys. Rev. B **77**, 115335 (2008).

[5] R. Rurali, B. Aradi, T. Frauenheim, and A. Gali, Phys. Rev. B **79**, 115303 (2009).

[6] Y. M. Niquet, L. Genovese, C. Delerue, and T. Deutsch, Phys. Rev. B **81**, 161301(R) (2010).

[7] Y. Cui, Q. Wei, P. Park, and C. M. Lieber, Science **293**, 1289 (2001).

[8] A. I. Boukai, Y. Bunimovich, J. Tahir-Kheli, J.-K. Yu, W. A. Goddard, and J. R. Heath, Nature (London) **451**, 168 (2008).

[9] B. Tian, X. Zheng, T. J. Kempa, Y. Fang, N. Yu, G. Yu, J. Huang, and C. M. Lieber, Nature (London) **449**, 885 (2007).

[10] G. Makov and M. C. Payne, Phys. Rev. B **51**, 4014 (1995).

[11] S. Lany and A. Zunger, Phys. Rev. B **78**, 235104 (2008).

[12] C. Freysoldt, J. Neugebauer, and C. G. Van de Walle, Phys. Rev. Lett. **102**, 016402 (2009).

[13] S. E. Taylor and F. Bruneval, Phys. Rev. B **84**, 075155 (2011).

[14] R. Rurali, M. Palummo, and X. Cartoixà, Phys. Rev. B **81**, 235304 (2010).

[15] S. Z. Sze, *Physics of Semiconductor Devices*, 2nd ed. (Wiley, New York, 1981).

[16] Y. Maeda, N. Tsukamoto, Y. Yazawa, Y. Kanemitsu, and Y. Masumoto, Appl. Phys. Lett. **59**, 3168 (1991).

[17] A. G. Cullis, L. T. Canham, and P. D. J. Calcott, J. Appl. Phys. **82**, 909 (1997).

[18] T.-L. Chan, Phys. Rev. B **86**, 245414 (2012).

[19] T.-L. Chan, S. B. Zhang, and J. R. Chelikowsky, Phys. Rev. B **83**, 245440 (2011).

[20] J. R. Chelikowsky, N. Troullier, and Y. Saad, Phys. Rev. Lett. **72**, 1240 (1994).

[21] J. R. Chelikowsky, J. Phys. D **33**, R33 (2000).

[22] L. Kronik, A. Makmal, M. L. Tiago, M. M. G. Alemany, M. Jain, X. Y. Huang, Y. Saad, and J. R. Chelikowsky, Phys. Status Solidi B **243**, 1063 (2006).

[23] J. Han, M. L. Tiago, T.-L. Chan, and J. R. Chelikowsky, J. Chem. Phys. **129**, 144109 (2008).

[24] N. Troullier and J. L. Martins, Phys. Rev. B **43**, 1993 (1991).

[25] S. G. Louie, S. Froyen, and M. L. Cohen, Phys. Rev. B **26**, 1738 (1982).

[26] A. J. Lee, M. Kim, C. Lena, and J. R. Chelikowsky, Phys. Rev. B **86**, 115331 (2012).

[27] S. P. Beckman, J. Han, and J. R. Chelikowsky, Phys. Rev. B **74**, 165314 (2006).

[28] D. M. Ceperley and B. J. Alder, Phys. Rev. Lett. **45**, 566 (1980).

[29] C. G. Broyden, IMA J. Appl. Math. **6**, 222 (1970).

[30] R. Fletcher, Comput. J. **13**, 317 (1970).

[31] D. Goldfarb, Math. Comp. **24**, 23 (1970).

[32] D. F. Shanno, Math. Comput. **24**, 647 (1970).

[33] Y. Wu, Y. Cui, L. Huynh, C. J. Barrelet, D. C. Bell, and C. M. Lieber, Nano Lett. **4**, 433 (2004).

[34] X. Y. Huang, E. Lindgren, and J. R. Chelikowsky, Phys. Rev. B **71**, 165328 (2005).

[35] J. Han, T.-L. Chan, and J. R. Chelikowsky, Phys. Rev. B **82**, 153413 (2010).

[36] T.-L. Chan, S. B. Zhang, and J. R. Chelikowsky, Appl. Phys. Lett. **98**, 133116 (2011).

[37] D. V. Melnikov and J. R. Chelikowsky, Phys. Rev. B **69**, 113305 (2004).

[38] Y. Zhou, Y. Saad, M. L. Tiago, and J. R. Chelikowsky, Phys. Rev. E **74**, 066704 (2006).

[39] D. V. Melnikov and J. R. Chelikowsky, Phys. Rev. Lett. **92**, 046802 (2004).

[40] T.-L. Chan, M. L. Tiago, E. Kaxiras, and J. R. Chelikowsky, Nano Lett. **8**, 596 (2008).

[41] J. B. McManus, R. People, R. L. Aggarwal, and P. A. Wolff, J. Appl. Phys. **52**, 4748 (1981).

[42] F. Bruneval, Phys. Rev. Lett. **103**, 176403 (2009).

[43] E. Kikuchi, S. Ishii, and K. Ohno, Phys. Rev. B **74**, 195410 (2006).

[44] G. M. Dalpian and J. R. Chelikowsky, Phys. Rev. Lett. **96**, 226802 (2006).